

Article

Multi-Objective Optimization-Based Health-Conscious Predictive Energy Management Strategy for Fuel Cell Hybrid Electric Vehicles

Mehdi Sellali ^{1,2,*}, Alexandre Ravey ¹, Achour Betka ², Abdellah Kouzou ^{3,4}, Mohamed Benbouzid ^{5,6}, Abdesslem Djerdir ¹, Ralph Kennel ⁷ and Mohamed Abdelrahem ^{7,8,*}

¹ FEMTO-ST Institute (UMR CNRS 6174), University of Technology of Belfort-Montbéliard, 90010 Belfort, France; alexandre.ravey@femto-st.fr (A.R.); abdesslem.djerdir@utbm.fr (A.D.)

² LGEB Laboratory, University of Biskra, Biskra 07000, Algeria; betkaachour@gmail.com

³ LAADI Laboratory, Faculty of Sciences and Technology, Ziane Achour University, Djelfa 17000, Algeria; kouzouabdellah@ieee.org

⁴ Electrical and Electronics Engineering Department, Nisantasi University, 34398 Istanbul, Turkey

⁵ Institut de Recherche Dupuy de Lôme (UMR CNRS 6027 IRDL), University of Brest, 29238 Brest, France; Mohamed.Benbouzid@univ-brest.fr

⁶ Logistics Engineering College, Shanghai Maritime University, Shanghai 201306, China

⁷ Chair of Electrical Drive Systems and Power Electronics, Technical University of Munich (TUM), 80333 Munich, Germany; ralph.kennel@tum.de

⁸ Faculty of Engineering, Assiut University, Assiut 71516, Egypt

* Correspondence: sellalimehdi5@gmail.com (M.S.); Mohamed.abdelrahem@tum.de (M.A.)

Citation: Sellali, M.; Ravey, A.; Betka, A.; Kouzou, A.; Benbouzid, M.; Djerdir, A.; Kennel, R.; Abdelrahem, M. Multi-Objective Optimization-Based Health-Conscious Predictive Energy Management Strategy for Fuel Cell Hybrid Electric Vehicles. *Energies* **2022**, *15*, 1318. <https://doi.org/10.3390/en15041318>

Academic Editors: Oscar Barambones and Jose Antonio Cortajarena

Received: 6 December 2021

Accepted: 7 February 2022

Published: 11 February 2022

Publisher's Note: MDPI stays neutral with regard to jurisdictional claims in published maps and institutional affiliations.



Copyright: © 2022 by the authors. Licensee MDPI, Basel, Switzerland. This article is an open access article distributed under the terms and conditions of the Creative Commons Attribution (CC BY) license (<https://creativecommons.org/licenses/by/4.0/>).

Abstract: The Energy Management Strategy (EMS) in Fuel Cell Hybrid Electric Vehicles (FCHEVs) is the key part to enhance optimal power distribution. Indeed, the most recent works are focusing on optimizing hydrogen consumption, without taking into consideration the degradation of embedded energy sources. In order to overcome this lack of knowledge, this paper describes a new health-conscious EMS algorithm based on Model Predictive Control (MPC), which aims to minimize the battery degradation to extend its lifetime. In this proposed algorithm, the health-conscious EMS is normalized in order to address its multi-objective optimization. Then, weighting factors are assigned in the objective function to minimize the selected criteria. Compared to most EMSs based on optimization techniques, this proposed approach does not require any information about the speed profile, which allows it to be used for real-time control of FCHEV. The achieved simulation results show that the proposed approach reduces the economic cost up to 50% for some speed profile, keeping the battery pack in a safe range and significantly reducing energy sources degradation. The proposed health-conscious EMS has been validated experimentally and its online operation ability clearly highlighted on a PEMFC delivery postal vehicle.

Keywords: energy management strategy; model predictive control; health conscious; multi-objective optimization; fuel cell hybrid electric vehicles

1. Introduction

Nowadays, global warming is considered a major problem that can cause serious environmental threat and may lead to social damage in the coming years. Therefore, environmental awareness must call for a reduction in both fuel consumption and emissions from conventional vehicles with Internal Combustion Engines (ICEs) [1]. To cope with this problem, new regulations must be taken, such as the restriction of unnecessary transportation activities and the development of Fuel Cell Hybrid Electric Vehicles (FCHEVs) [2]. Among all current solutions, FCHEVs are one of the most promising approaches to achieve significant reductions in both fuel consumption and greenhouse gas emissions

[3]. A FCHEV uses a Proton-exchange Membrane Fuel Cell (PEMFC) as a primary source, an Energy Storage Source (ESS), such as lithium ion batteries, or Supercapacitors (SCs) as a secondary source, an Electric Motor (EM) and inverter(s). Different types of FCHEVs have been developed. They are divided into passive, semi active, and active configuration [4]. FCHEVs are multi-source systems where a complex power flow needs to be managed. Thus, an improvement in the hydrogen economy needs to be considered. For this purpose, advanced control algorithms, called Energy Management Strategies (EMSs) are designed to control the power distribution [5]. The EMS decides how to share the demanded power among the different power sources to maintain auxiliary source state of charge, optimize powertrain efficiency, and reduce fuel consumption [6]. Over the past few decades, the common-used EMSs for FCHEVs can be divided into two types, Rules-based Strategies (RBSs) and Optimization-based Strategies (OBS) [7]. An RBS is a real-time control THAT depends on the vehicle parameters, the power demanded by the EM, and the auxiliary source State of Charge (SOC) [8]. These rules are divided into Deterministic Strategies (DRs) and Fuzzy Logic strategies (FLs). DRs are based on certain FCHEV parameters, such as the battery power threshold, the SOC, the nominal PEMFC power, and the SCs reference voltage [9]. Conversely, FRs are defined according to engineer experience. The variables should be fuzzified and defuzzified during several tests [10,11]. However, FRs is more adaptable to different operating modes compared to DRs. For instance, the RBS performance is affected by the set rules parameters and will be far from the optimal operating conditions. For example, after several cycles, the calculation of PEMFC hydrogen consumption will become increasingly inaccurate over time due to the parametric variation of the fuel cell. Therefore, the EMS is established on the basis of fixed parameters, which will lead to a mismatch between the calculation result and actual results [12]. For this purpose, a new RBS combined with Dynamic Programming (DP) is proposed in [13], where a maximum power demand determines the power required by each source based on the estimation of the real parameters of the PEMFC, and it effectively reduces fuel consumption. The EMS based on the OBS are divided into Global Optimization Rules (GORs) or offline rules and Instantaneous Optimization Rules (IORs). The IORs are also called real-time optimization rules [14]. OBSs are used to minimize a cost function, which usually reflects the fuel consumption over a fixed driving cycle. Usually, they are based on the knowledge of past or future power demands, such as the Pontryagin Minimum Principle (PMP) [15], metaheuristic approaches [16], and Genetic Algorithm (GA) [17]. Many studies on OBS have been proposed by using a weighted sum of a multi-objective function [18], which can be used to solve the problem offline. However, the computation burden remains an inconvenience. In addition, most EMS algorithms focus on a specific optimization objective, such as minimizing fuel consumption or improving efficiency. In order to achieve the overall optimal solution, a stochastic predictive algorithm based on fast rolling optimization has been developed in [19]. In combination with a large amount of data, the torque of the EM and EMS are modeled using Markov chains. However, the energy must be calculated off-line and the driving cycle must be known in advance. Nevertheless, this strategy requires considerable fine-tuning to achieve the best control gains. A hierarchical control based on the equivalent fitting circle method is adopted in [20] to achieve optimal power sharing. The power of each PEMFC is determined using a mathematical model to solve the power output. Nevertheless, for different PEMFCs with different models and parameters, this method is clearly not sufficient, particularly with the increase in the number of FC. DP is a model-based technique that seeks all control states in order to have an optimal control strategy [21,22]. However, this technique is not suitable for real-time problems since the exact information about the future driving is unknown. The lifetime of the ESS in a FCHEV is very sensitive to their operation, knowing how to coordinate the two energy units to reduce the fuel consumption, as well as preserving their degradations presents another challenge [23]. Several improved EMSs can be found in the literature, such as the Extreme Seeking (ES) method [24], Q-Learning and Neuro-Dynamic Programming [25], robust control [26], or Reinforcement Learning (RL) method

[27]. By analyzing the previous limited literature, it can be noted that offline optimization algorithms are difficult to operate in real time applications and are time consuming. Most of the existing works on FCHEVs examine the minimization of hydrogen consumption, without implying the performance degradation of energy sources, thus the economic potential of FCHEVs is not really assessed. In [28], the authors introduced a battery SOH-sensitive technique applied to the powertrain. The authors have shown that this work reduced overall battery degradation while limiting the impact on the fuel economy, leading to a reduction in total vehicle price. In [29], an ES conducted on a FCHEV showed that it significantly extended the battery life for the US06 cycle. Another EMS was successfully performed in [30], where it saved about 15,000 Euros using the same battery pack for the entire life of the bus. Other examples of online EMSs, which are sensitive to battery ageing, have included convex optimization [31], and model-based predictive control [32–34]. These efforts have shown that perceptive EMSs based on battery State of Health (SOH) can offer significant economic benefits. However, most of recent works have made the SOC to fluctuate freely. In this work, battery SOC regulation is a key point in tracking where the costs associated with the sources represent a significant rate of the total vehicle cost. Depending on the type of hybrid sources, this cost can reach 70% of the vehicle price [35,36]. In this sense, it makes sense to include health awareness in the EMSs. The MPC rules have been widely used for EMS in the automotive control because of its ability to deal with real time optimization applications. Several EMSs based on MPC have been developed, however none discuss the sources degradation. In order to fill this gap, this article presents an original contribution that will improve the lithium-ion battery lifetime and preserve the PEMFC dynamics in a cost-healthy manner; the main contributions of this article consist of the following points:

- A proposed objective function formulated within the MPC framework that minimizes the hydrogen cost, preserves FC dynamics, and extends the lithium-ion battery lifespan;
- A semi-active topology is proposed where the MPC deal with the severe nonlinearities and the time-varying property of a FCHEV;
- A comparative study between the proposed method and a Fuzzy Logic (FL) method is conducted using three different driving cycles in simulation, followed by experimental validation using a test protocol.

The remaining part of the paper is organized as follows. The FCHEV powertrain model is presented in Section 2. In Section 3, the health-conscious EMS based on the MPC framework is presented in detail. The simulation results under various driving cycles are presented in Section 4, followed by the implication of power-source pricing. The Experimental results and analysis are introduced in Section 5. Finally, Section 6 presents the conclusion.

2. FCHEV Modeling

The investigation presented in this paper is based on an electrical vehicle Moby Post, which has been developed by the European project Moby Post. Its semi-active architecture of the Moby Post vehicle is shown in Figure 1. The PEMFC is the main power source that provides the steady-state power. It is powered by an integrated hydrogen tank and is connected to a DC/DC unidirectional boost converter that continuously feeds the DC bus link while, the battery is directly connected to the DC link to maintain its voltage. The DC link is connected to two inverters controlling the two-wheel motors. For the system supervision, an Electronic Control Unit (ECU) is used so that it communicates with all the dedicated controllers of the different subsystems via a CAN bus network. The addition of the battery as an auxiliary power source is intended to protect the PEMFC and improve the performance of FCHEV.

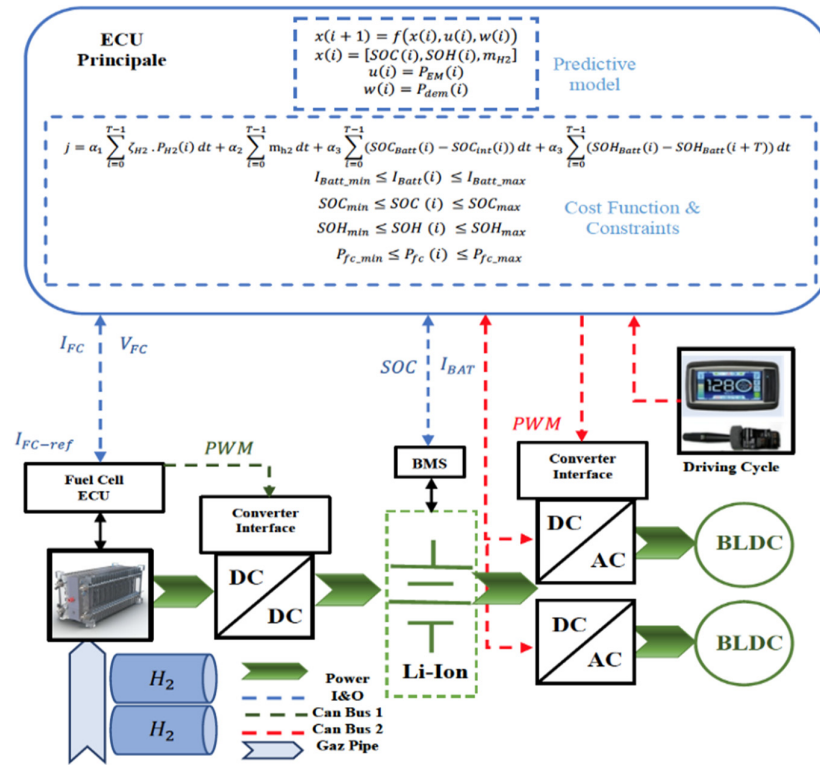


Figure 1. Synoptic diagram of the Moby Post vehicle.

The power needed from the vehicle to meet the speed requirements of the driving cycle can be calculated using the dynamic model of the vehicle. All the parameters of the vehicle are presented in the Appendix. This power is supplied by the PEMFC and the lithium-ion battery according to the following equations:

$$M \frac{dv}{dt} = \sum F_t - \sum F_r \quad (1)$$

$$P_{dem}(w) = P_{PEMFC} \cdot \eta_{DC/DC} + P_{Batt}. \quad (2)$$

V represents the vehicle speed, F_t represents the sum of the vehicle's traction forces, F_r represents the total resistive forces, M represents the vehicle mass, P_{dem} represents the demanded power, and $\eta_{DC/DC}$ represents the efficiency of the unidirectional Boost converter.

2.1. PEMFC Model

The voltage of a single cell is very low (between 0.4 and 1 V), far from sufficient voltage to power the vehicle. This is why the PEMFC is designed in a stack to provide continuous power with a reasonable voltage [37]. The stack voltage can be calculated by simply multiplying the number of cells and the voltage of a single cell according to the following equation:

$$V_{PEMFC} = N_{cell} \cdot V_{cell} \quad (3)$$

where V_{PEMFC} is the PEMFC voltage, N_{cell} is the number of cells in the stack, and V_{cell} is the voltage of a single cell. The electrochemical process within the PEMFC is associated with many losses, and these losses are activation losses, ohmic losses, and concentration losses. The voltage produced by the PEMFC cell is calculated by subtracting those losses from the reversible thermodynamic voltage E_{rev} [38]. The output voltage can be expressed as follows:

$$V_{cell} = E_{rev} - V_{irrev} \quad (4)$$

$$V_{irrev} = V_{act} - V_{ohm} - V_{con} \quad (5)$$

V_{act} are the activation losses due to the activation reactions of the anode and cathode, V_{ohm} are the ohmic losses related to the conduction of protons through the solid electrolyte and electrons through the internal resistance, and V_{con} are the concentration losses due to the mass transport of the reacted gases [39]. The reversible thermodynamic potential is the voltage that would be obtained if all the energy of the electrochemical reaction was converted into electricity without any loss. It can be calculated from the following equation [40].

$$E_{rev} = E_0 + \frac{R \cdot T}{n \cdot F} \ln \left(\frac{\prod_i a_{reactant_i}}{\prod_j a_{product_j}} \right) \quad (6)$$

Where i and j are the numbers of reactant types and products; $a_{reactant_i}$ and $a_{product_j}$ are the reactant and partial pressure of the product [atm], R is the universal gas constant, F is the Faraday constant, n is the number of electrons transferred for each molecule of the fuel participating in the reaction, and T is the temperature in Kelvin [K]. The PEMFC adopted in this vehicle is the H-3000 with a nominal power of 1 kW, its parameters are presented in the Appendix. The hydrogen consumption is the amount of hydrogen that is actually consumed in the PEMFC reaction and can be calculated as follows [41]:

$$\dot{m}_{h_2} = \frac{N_{cell} \cdot M_{h_2}}{s \cdot F} I_{stack} \cdot \lambda \quad (7)$$

where \dot{m}_{h_2} is the hydrogen mass flow rate (g/s), N_{cell} is the number of cells, M_{h_2} is the molar mass of hydrogen (g/mol), s is the active surface of each cell, F is the Faraday constant, and λ is the ratio of excess hydrogen.

2.2. Lithium Ion Battery Model

The battery is the vehicle auxiliary ESS where a first-order model is adopted in this paper. Compared to the multi-physical and empirical model, this model cannot only ensure a reduced computation time but also meet high accuracy requirements. This model is shown in Figure 2 [42,43]. In addition, the voltage drop is related to the current and ohmic resistance R_s . The voltages V_s and V_1 refer, respectively, to the series resistance and the concentration polarization voltage C_1 , and finally, the voltage at the terminals of the battery V_B is expressed as follows [44]:

$$V_B = E_0 - R_s \cdot I_B - V_1 \quad (8)$$

The state of charge can be defined as follows:

$$SOC(k) = SOC(k) - \frac{i(k)dt}{Q} \quad (9)$$

where SOC , Q , and dt are respectively the cell state of charge, the nominal capacity of the cell, and the sampling interval.

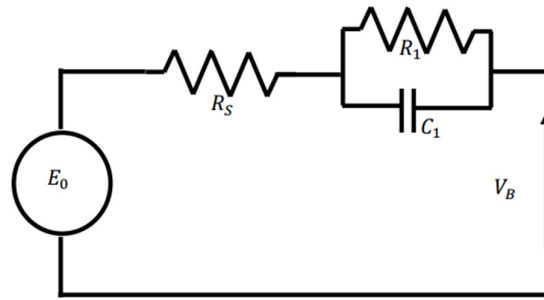


Figure 2. Equivalent lithium-ion circuit model.

2.3. Battery Degradation Model

In the literature, several models have been presented to describe the degradation phenomena of lithium-ion batteries [45–48]. The most significant model for evaluating the capacity loss of lithium-ion batteries is the exponential one. It is described as follows:

$$Q_{loss} = B(c) \cdot \exp\left(\frac{-E_a(c)}{RT}\right) \cdot A(c)^z \quad (10)$$

where Q_{loss} is the loss percentage (%) of the battery capacity, c is the capacity in (Ah), B is the exponential factor, T is the absolute temperature in K, and R is the gas constant (8.31 J/mol·K). The other parameters of the capacity loss model were obtained experimentally from a large set of test data. The activation energy E_a in (J/mol) and the power-law factor z are given as follows:

$$\begin{cases} E_a(c) = 31700 - 370 \cdot c \\ z = 0.55 \end{cases} \quad (11)$$

A drop in capacity of up to 20% of rated capacity is considered to be the end-of-life capacity of the lithium-ion batteries, so that the total Ah over the set of A is expressed as follows:

$$A = \left(\frac{20}{B(c) \exp\left(\frac{-E_a(c)}{RT}\right)} \right)^{\frac{1}{z}} \quad (12)$$

Assuming a symmetrical capacity during the charging and discharging process, the battery charge can be determined as follows:

$$N = \frac{3600 \cdot A}{Q_{cell}} \quad (13)$$

where Q_{cell} indicates the nominal capacity of the battery in As. The health model can be calculated as follows:

$$SOH(t) = 1 - \frac{\int_0^t |I_{Batt}(t)| dt}{2N \cdot Q_{cell}} \quad (14)$$

where I_{Batt} is the charging current of the battery. Note that the initial value of SOH is assumed to be 1. The rate of change of SOH can be derived as:

$$SOH(k+1) = SOH(k) - \frac{|I_{Batt}(t)| dt}{2N \cdot Q_{cell}} \quad (15)$$

In the case where the actual conditions do not correspond to those given by the current manufacturer, several methods have been proposed for hybrid vehicles to estimate the battery life [49,50]. They are based on the concept of Ah charge quantity, which assumes that there is an amount of accumulated charge that can flow through the battery (in a charge or discharge situation) before it reaches its End of Life (EOL).

3. Health Conscious-Based EMS for FCHEV

In this hybrid system, the average power is given by the PEMFC because of its slow dynamics, while the higher power limit is given by the battery pack to recover kinetic energy during deceleration and to ensure rapid acceleration. The health-conscious predictive supervisor has to adjust the power dynamics according to the PEMFC reference current and maintains the battery SOC at its initial value. It has been proven in [51] that the ON/OFF operation has a negative impact on the PEMFC lifetime. To take this effect into account, we therefore prefer that the PEMFC remains active during the entire delivery period. Since the required energy is supported by the battery pack and the PEMFC, the predictive supervisor used for this study is designed to meet several objectives:

- Minimize fuel consumption,
- Preserve the PEMFC dynamic,
- Keep the SOC of the lithium-ion battery at the same level as the initial value,
- Preserve the lithium-ion battery pack.

The proposed objective function is based on the finite horizon iterative optimization, whereas, the prediction horizon must cover the control sequences that represent here the PEMFC current values (1–50 A). After having the optimal PEMFC current value, which is the only degree of freedom in this control algorithm, the model will be predicted again and the control sequences evaluated according to this objective function:

$$j = \alpha_1 \sum_{i=0}^{T-1} \zeta_{H2} \cdot P_{fc}(i) dt + \alpha_2 \sum_{i=0}^{T-1} m_{h2} dt + \alpha_3 \sum_{i=0}^{T-1} (SOC_{Batt}(i) - SOC_{int}(i)) dt + \alpha_4 \sum_{i=0}^{T-1} (SOH_{Batt}(i) - SOH_{Batt}(i + T)) dt. \quad (16)$$

T is the interval of the prediction/control horizon, ζ_{H2} is the price of hydrogen per Joule, P_{fc} is the PEMFC power, m_{h2} is the hydrogen consumption, and SOC_{Batt} and SOH_{Batt} are the state of charge and battery state of the health, respectively. The constraints to be satisfied to solve this optimization process over T can be mathematically formulated as follows:

$$SOC(i + 1) = SOC(i) - \frac{I_{Batt}(i) \Delta t}{Q} \quad (17)$$

$$I_{Batt_min} \leq I_{Batt}(i) \leq I_{Batt_max} \quad (18)$$

$$SOC_{min} \leq SOC(i) \leq SOC_{max} \quad (19)$$

$$SOH(i + 1) = SOH(i) - \frac{|I_{Batt}(i)| \Delta t}{2 \cdot N \cdot Q} \quad (20)$$

$$SOH_{min} \leq SOH(i) \leq SOH_{max} \quad (21)$$

$$P_{fc_min} \leq P_{fc}(i) \leq P_{fc_max} \quad (22)$$

where the output of the predictive supervisor is the PEMFC reference current. It is worth noting that the choice of the appropriate horizon size is an essential step that must involve a compromise between optimality and computational efficiency. As the size of the horizon becomes larger, the total cost of operation decreases, while the computing load increases.

The minimization process of the objective function was made by the Sequential Quadratic Programming (SQP) algorithm; the interest of using this algorithm is its effectiveness in several previous works on MPC-based EMS. SQP is a nonlinear iterative optimization method with constraints. It is usually used for mathematical problems for which the objective function and the constraints are continuously differentiable. This approach solves a sequence of optimization subsets, each of these subsets are optimizing a quadratic model of the objective function under constraints. The weighting factors were selected by giving the same importance to the four terms to be optimized, which leads to set the four factors equal to 0.25. As a result, all the weighting factors are equalized, eliminating the need to adjust them online. The equal-weighted cost function not only provides simplicity in the MPC design, but also guarantees the desired controller performance.

4. Simulation Results and Discussions

A speed profile is a series of data representing the speed of a vehicle as a function of time. Speed profiles are produced by different countries and organizations to evaluate vehicle performance in a variety of ways, such as fuel consumption and pollutant emissions. The speed profile used in this study are shown in Figure 3.

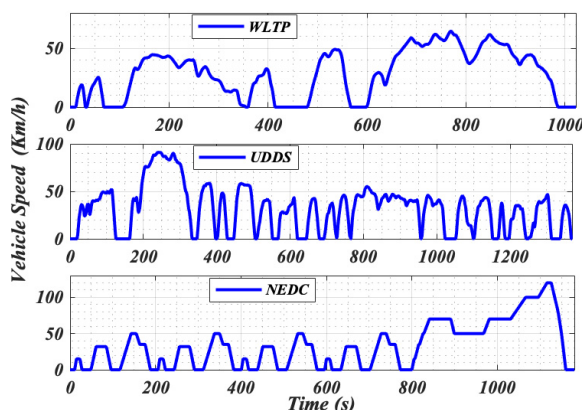


Figure 3. Speed profiles.

4.1. Driving Cycles

The three speed profiles adopted are the World wide harmonized Light vehicles Test Procedures (WLTP), the Urban Dynamometer Driving Program (UDDS), and the New European Driving Cycle (NEDC), in order to analyze the performance of the proposed healthy EMS. All speed profiles take place on a flat track.

4.2. Comparison Results

This paper aims to compare the proposed algorithm with a baseline technique, which is the Fuzzy Logic method [21]. In the latter, Alexander et al. focused on maintaining the SOC of the battery in an optimal zone (around 0.7). Conversely, to reduce hydrogen consumption, the membership function defining the PEMFC current is trapezoidal and each has four variables (zero, low optimal, and high). The simulation results are presented to evaluate the effectiveness of the proposed healthy EMS. In detail, the simulations are performed in the MATLAB/Simulink environment for 3 speed profiles. The baseline method does not take into account the degradation of lithium-ion batteries, while the proposed method implements a healthy EMS that respect the battery degradation and PEMFC dynamics. The distribution of the power between the PEMFC and battery is illustrated in Figures 4–6. It is clear that for the predictive supervisor, the PEMFC is used to provide the permanent part of the required power in a stable manner, while the battery is mainly responsible for absorbing and providing fast transitions. It can also be seen that the PEMFC powers are efficiently smoothed by the battery during the whole driving cycle, in this case the negative values of the battery power, which means that the recovered braking energy can recharge the battery. It also appears from these figures that the proposed strategy is capable of limiting the operation of the fuel cell to the nominal power where the maximum efficiency is reached, i.e., about 50 A, most of the time.

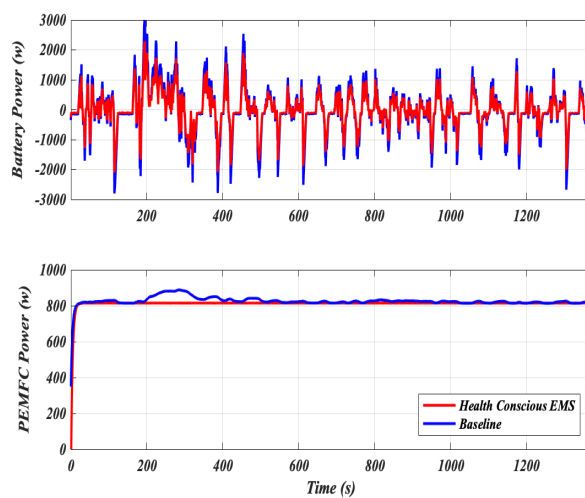


Figure 4. PEMFC and battery power for the UDDS cycle.

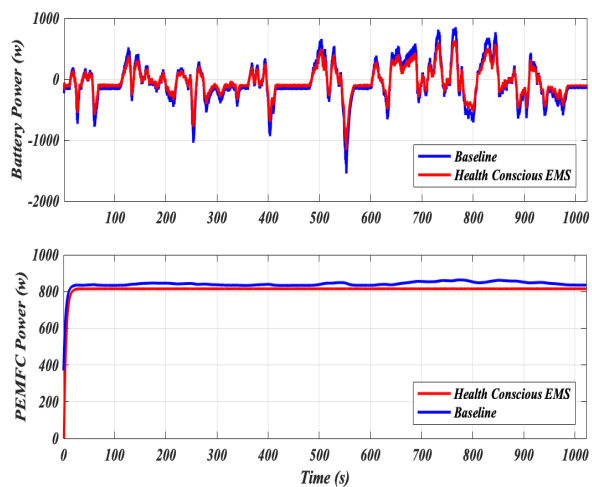


Figure 5. PEMFC and battery power for the WLTP cycle.

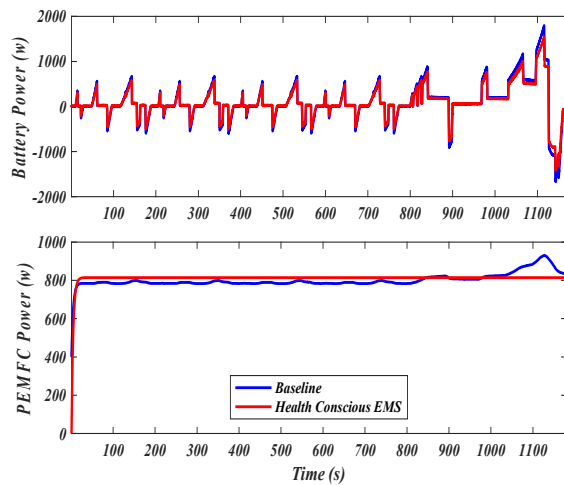


Figure 6. PEMFC and battery power for the NEDC cycle.

Figures 7–9 shows the curves of the battery states of charge and health states according to the two strategies, in which the SOC varies from 0.6 to 0.5852 for the baseline technique, and it remains constant at 0.6 for the proposed technique. The FL technique does not take into account the SOC's maintenance capacity, which results in a decrease in the SOC, however, since the SOC is included in the objective function, the SOC can return to its initial state. It can be seen that the proposed healthy EMS works well to ensure that the battery's state of charge is maintained with a slight decrease in SOH of less than 0.005%. On the other hand, the PEMFC is used too aggressively in the baseline technique, which lead to reaching the EOL much earlier than the proposed method. By plotting the battery degradation graph at (Figure 10), it can be seen that the healthy EMS reduced battery degradation and extended battery life by about 40%. Therefore, it can be concluded that there is a need to consider the health of the system. It should also be noted that when the sources reach a high level of degradation, the predictive supervisor must readjust the PEMFC reference current adequately to avoid further degradation.

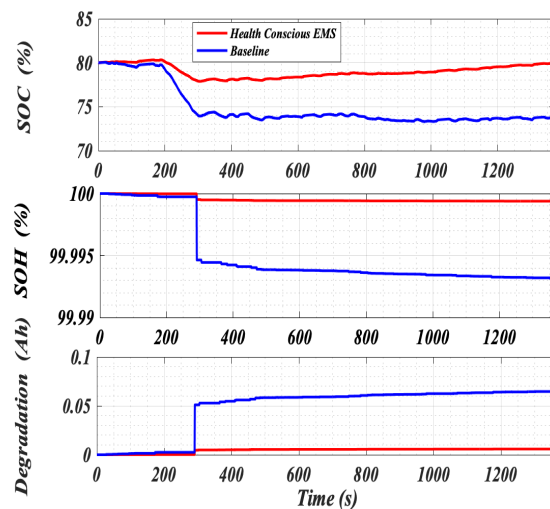


Figure 7. Battery SOC, SOH, and degradation for the UDDS cycle.

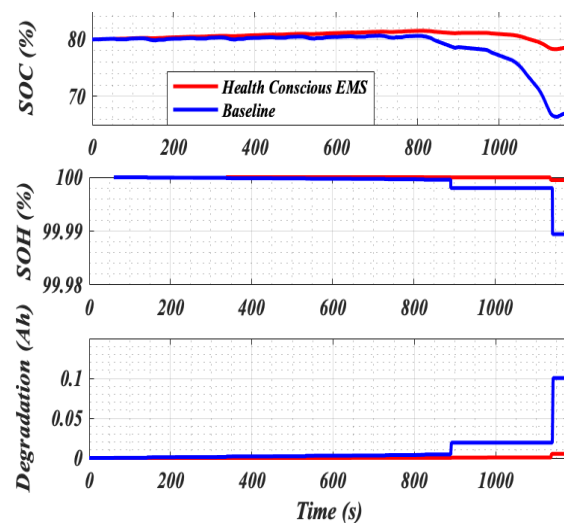


Figure 8. Battery SOC, SOH, and degradation for the WLTP cycle.

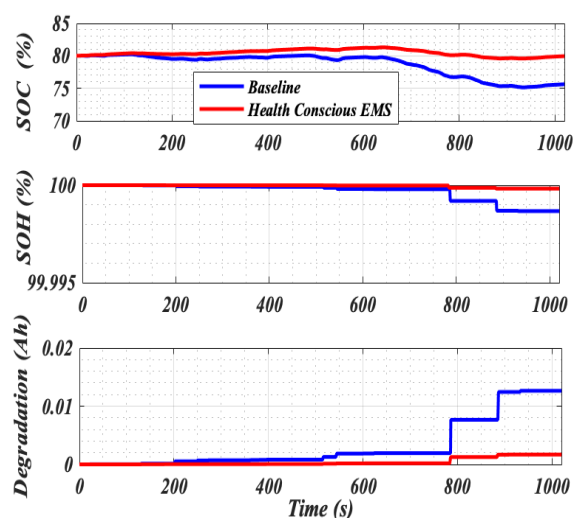


Figure 9. Battery SOC, SOH, and degradation for the NEDC cycle.

The healthy EMS shows better fuel economy performance than the baseline technique. We can observe an average 20% reduction in fuel consumption over the three cycles. In the above discussion, we examine the impact of cost on the two EMSs, considering that the price of hydrogen is 3.57 \$/Kg [35]. The global hydrogen consumption after repeating the cycles 8 times for the two strategies are shown in Table 1, which are 1.36 Kg, 2.07 Kg, and 1.78 Kg, respectively for the baseline strategy and 1.09 Kg, 1.56 Kg, and 1.34 Kg for the health-conscious strategy. The increase of hydrogen consumption is estimated to change from 20% to 25%, due to the PEMFC power variation for the baseline technique. This means a significant benefit while using the proposed method in terms of hydrogen price. These prices are decreased by 26%, 50%, and 43% for WLTP, UDDS, and NEDC, respectively.

Table 1. Performance comparison.

| Cycles | Fuel Consumption (Kg/8 Cycles) | | | Cost (3.75 €/Kg) | | |
|--------|-----------------------------------|------|-------------|---------------------|------|---------|
| | Baseline | MPC | Improvement | Baseline | MPC | Benefit |
| WLTP | 1.36 | 1.09 | 20.01% | 4.85 | 3.89 | 0.96 |
| UDDS | 2.07 | 1.56 | 24.50% | 7.38 | 5.56 | 1.82 |
| NEDC | 1.78 | 1.34 | 25% | 6.35 | 4.78 | 1.57 |

The results of the proposed technique for the three cycles show clearly that hydrogen costs are significantly reduced. These results clearly showed that, without taking into account the degradation criteria, the baseline technique will be very expensive for the post delivery. The results could be considered as an excellent optimal solution for other types of FCHEVs.

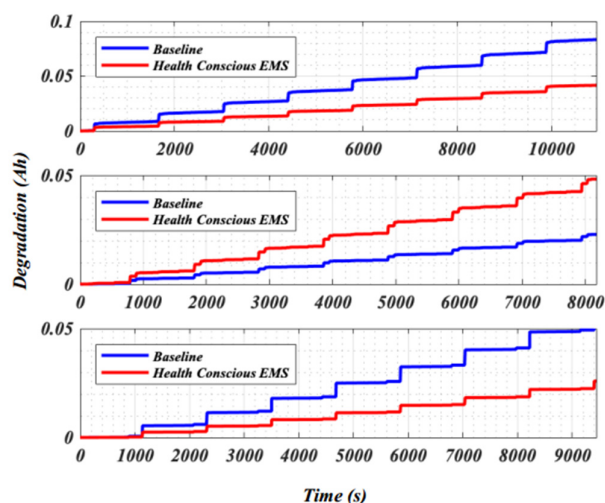


Figure 10. Degradation comparison.

5. Real-Time Assessment

In order to verify the effectiveness of the proposed EMS, the experiment is carried out on the Moby Post vehicle as shown in Figure 11. The PEMFC used in this work is AIRCELL1000 ACS, which is fed by an embedded hydrogen tank and connected to a DC/DC boost converter, which provides a permanent supply to the vehicle. For the Energy Storage System (ESS), four lithium-ion battery modules have been used. Each single module is able to deliver a power of 2 kW constantly with a nominal voltage of 13.4 V. These modules are connected directly to the DC bus link to maintain it at 50 V. A Battery Management System (BMS) is connected to the battery pack, this latter provides safety functions that protect the battery pack automatically by disconnecting it from the high load current as well as balancing the voltages of each module. A classic DC/DC boost converter has been used in order to interface the PEMFC and DC bus link due to the low PEMFC stack voltage. This DC/DC is designed by Zahn Electronics with a nominal power of 1.7 kW. For the supervision and energy management of the system, an Electronic Control Unit (ECU) designed by “FAAR Industry” is used in such a way that it communicates with all dedicated controllers of the different subsystems using a CAN bus network. The data has been recorded using the DRU908 developed by “ISAAC Instruments”. This communication bus allows access to the data of 130 vehicles such as speed, GPS position, etc. A test protocol has been established in the UTBM parking lot. The test was carried out not only to validate the proposed health-conscious EMS, but also to demonstrate its ability to operate in real time on an embedded system. The data were recorded using the DRU908 developed by “ISAAC Instruments”. This communication bus allows access the data of 130 vehicles, regarding speed, GPS position, etc. The parameters of the Moby Post FCHEV are summarized in the Appendix A.



Figure 11. Moby Post FCHEV.

The test protocol of the Moby Post vehicle working condition is shown in Figure 12, with the speed profile containing high acceleration and deceleration as well as many stops, which is similar to the postal delivery mission. Figure 12 shows that the real-time experimental results have the same shape as the simulation results. Thus, it can be concluded that after the driving cycle, the SOC converts to the initial value in order to start a new delivery mission. It can be concluded from Figure 13 that the proposed health-conscious predictive EMS has a strong capability to limit the PEMFC power dynamics and ensure that this latter provides power around its optimal point. In order to protect the PEMFC, the high-frequency components of the demanded power are provided by the battery pack, which give a good overview of the power fluctuation of PEMFC and highlight the advantages of the proposed technique. Moreover, it can be observed that when the vehicle accelerates, the battery pack reacts immediately and supplies the transient energy demand in a short time as displayed in the power curve of Figure 13, whereas the PEMFC slowly provides a power amount to adjust the battery SOC.

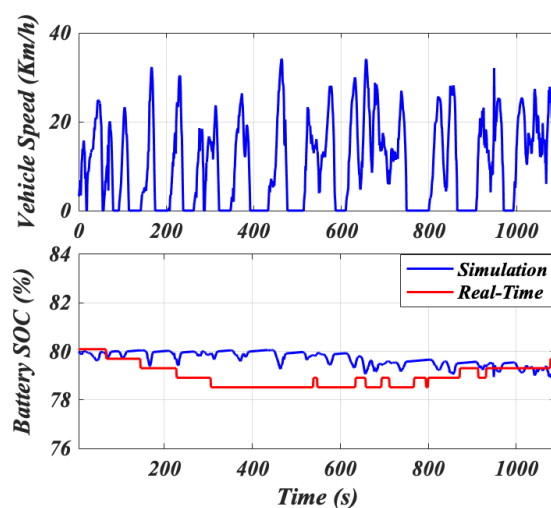


Figure 12. Real-time results of the speed profile and the battery SOC.

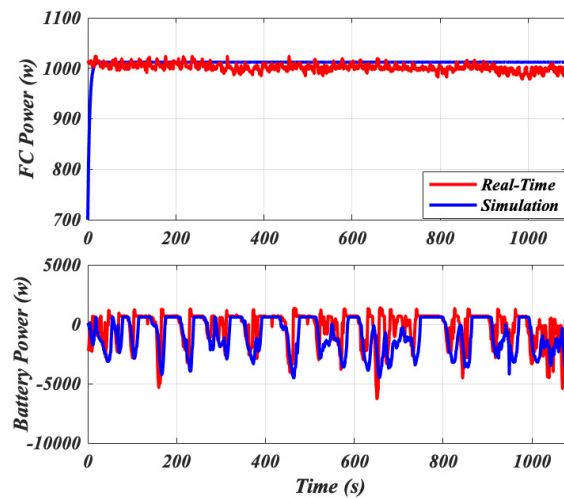


Figure 13. Real-time results of the PEMFC power and the battery power.

It can be also observed that the real-time experimental results show an exact conformity with the simulation results which validate the proposed technique. From the curve above (see Figure 14), it can be seen that the real-time experimental results of the hydrogen flow are similar to the simulation results, with the exception of some fluctuation in real-time due to the sensor sensitivity.

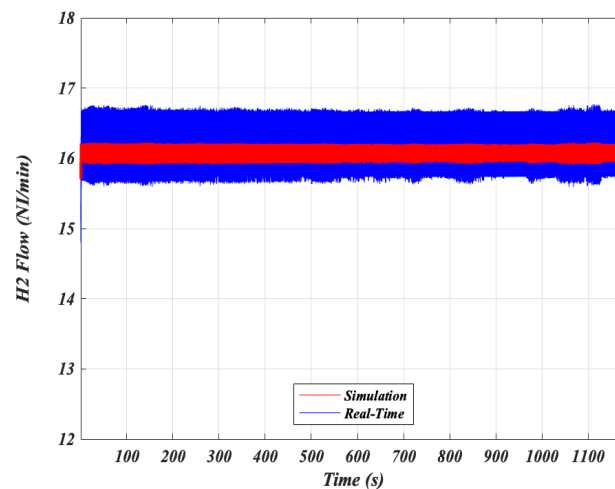


Figure 14. Hydrogen flow.

6. Conclusions

This paper proposed a health-conscious EMS for FCHEV. The proposed approach took into account the lithium-ion degradation, preserved the PEMFC dynamic, minimized the hydrogen consumption, and regulated the lithium-ion SOC. Simulation and real-time experimental results proved that the proposal is an alternative choice to developing cost-effective EMSs. Indeed, up to 25% of fuel consumption was achieved compared to baseline EMSs. Finally, the lithium-ion battery lifetime was extended, with its degradation reduced to 50%. It can be concluded that the proposed health-conscious EMS could be a promising solution for FCHEV confronting real constraints to enhance its performances in terms of reducing the degradations of its internal sources and increasing their lifespan, and therefore decreasing the overall costs of using FCHEV so as to be more competitive to conventional vehicles.

Author Contributions: Conceptualization, M.S., A.R., A.B., and A.K.; methodology, M.S., A.R., A.B., A.K., M.B., and A.D.; software, M.S., A.R., and A.B.; validation, M.S., A.B., A.K., and A.D.; formal analysis, M.S., A.K., and M.A.; investigation, M.S., A.B., A.K., and M.A.; resources, M.S., A.R., A.B., and A.K.; data curation, M.S., A.D., M.B., and A.K.; writing—original draft preparation, M.S., A.K., and M.A.; writing—review and editing, A.K., M.A., and R.K.; visualization, M.S., A.K., and M.A.; supervision, A.K., R.K., and M.A.; project administration, A.K., M.A., and R.K.; funding acquisition, M.A. and R.K. All authors have read and agreed to the published version of the manuscript.

Funding: This research received no external funding.

Institutional Review Board Statement: Not applicable.

Informed Consent Statement: Not applicable.

Data Availability Statement: Not applicable.

Acknowledgments: This work was supported by the German Research Foundation (DFG) and the Technical University of Munich (TUM) in the framework of the Open Access Publishing Program.

Conflicts of Interest: The authors declare no competing interest.

Appendix A

Total mass of the vehicle (kg) 530.

Coefficient of rolling resistance 0.02.

Aerodynamic drag coefficient 0.8.

Frontal area of vehicle (m^2) 2.56.

Gravitational force (m/s^2) 9.8.

Air density (Kg/m^3) 1.25.

References

1. Lakshminarayanan, V.; Chemudupati, V.G.S.; Pramanick, S.K.; Rajashekara, K. Real-time optimal energy management controller for electric vehicle integration in workplace microgrid. *IEEE Trans. Transp. Electrification* **2019**, *5*, 174–185.
2. Balali, Y.; Stegen, S. Review of energy storage systems for vehicles based on technology, environmental impacts, and costs. *Renew. Sustain. Energy Rev.* **2021**, *135*, 110185.
3. Snoussi, J.; Elghali, S.B.; Benbouzid, M.; Mimouni, M.F. Auto-adaptive filtering-based energy management strategy for fuel cell hybrid electric vehicles. *Energies* **2018**, *11*, 2118.
4. Das, H.S.; Tan, C.W.; Yatim, A.H.M. Fuel cell hybrid electric vehicles: A review on power conditioning units and topologies. *Renew. Sustain. Energy Rev.* **2017**, *76*, 268–291.
5. Fernandez, A.M.; Kandidayeni, M.; Boulon, L.; Chaoui, H. An adaptive state machine based energy management strategy for a multi-stack fuel cell hybrid electric vehicle. *IEEE Trans. Veh. Technol.* **2019**, *69*, 220–234.
6. Boukoberine, M.N.; Zhou, Z.; Benbouzid, M.; Donato, T. Frequency separation-based power management strategy for a fuel cell-powered drone. In Proceedings of the 2020 2nd International Conference on Smart Power Internet Energy Systems (SPIES), Bangkok, Thailand, 15–18 September 2020; pp. 209–214.
7. Sulaiman, N.; Hannan, M.A.; Mohamed, A.; Ker, P.J.; Majlan, E.H.; Daud, W.R.W. Optimization of energy management system for fuel-cell hybrid electric vehicles: Issues and recommendations. *Appl. Energy* **2018**, *228*, 2061–2079.
8. Sellali, M.; Betka, A.; Djerdir, A. Power management improvement of hybrid energy storage system based on h control. *Math. Comput. Simul.* **2020**, *167*, 478–494.
9. Li, Q.; Su, B.; Pu, Y.; Han, Y.; Wang, T.; Yin, L.; Chen, W. A state machine control based on equivalent consumption minimization for fuel cell/ supercapacitor hybrid tramway. *IEEE Trans. Transp. Electrification* **2019**, *5*, 552–564.
10. Sellali, M.; Abdeddaim, S.; Betka, A.; Djerdir, A.; Drid, S.; Tiar, M. Fuzzy-super twisting control implementation of battery/super capacitor for electric vehicles. *ISA Trans.* **2019**, *95*, 243–253.
11. Sellali, M.; Betka, A.; Drid, S.; Djerdir, A.; Allaoui, L.; Tiar, M. Novel control implementation for electric vehicles based on fuzzy-back stepping approach. *Energy* **2019**, *178*, 644–655.
12. Unger, J.; Kozek, M.; Jakubek, S. Nonlinear model predictive energy management controller with load and cycle prediction for non-road HEV. *Control Eng. Pract.* **2015**, *36*, 120–132.
13. Peng, J.; He, H.; Xiong, R. Rule based energy management strategy for a series-parallel plug-in hybrid electric bus optimized by dynamic programming. *Appl. Energy* **2017**, *185*, 1633–1643.
14. Sellali, M.; Betka, A.; Drid, S.; Djerdir, A.; Malik, O.P. Hardware implementation of an improved control strategy for battery-supercapacitor hybrid system in electric vehicles. *IET Electr. Syst. Transp.* **2020**, *10*, 204–212.
15. Mamun, A.; Liu, Z.; Rizzo, D.M.; Onori, S. An integrated designed control optimization framework for hybrid military vehicle using lithium-ion battery and supercapacitor as energy storage devices. *IEEE Trans. Transp. Electrification* **2019**, *5*, 239–251.

16. Trovao, J.P.F.; Santos, V.D.N.; Antunes, C.H.; Pereirinha, P.G.; Jorge, H.M. A real-time energy management architecture for multisource electric vehicles. *IEEE Trans. Ind. Electron.* **2014**, *62*, 3223–3233.
17. Lü, X.; Wu, Y.; Lian, J.; Zhang, Y.; Chen, C.; Wang, P.; Meng, L. Energy management of hybrid electric vehicles: A review of energy optimization of fuel cell hybrid power system based on genetic algorithm. *Energy Convers. Manag.* **2020**, *205*, 112474.
18. Serrao, L.; Onori, S.; Rizzoni, G. Ecms as a realization of pontryagin's minimum principle for HEV control. In Proceedings of the 2009 American Control Conference, St. Louis, MO, USA, 10–12 June 2009; IEEE: Manhattan, NY, USA, 2009; pp. 3964–3969.
19. Yang, C.; You, S.; Wang, W.; Li, L.; Xiang, C. A stochastic predictive energy management strategy for plug-in hybrid electric vehicles based on fast rolling optimization. *IEEE Trans. Ind. Electron.* **2019**, *67*, 9659–9670.
20. Yan, Y.; Li, Q.; Chen, W.; Huang, W.; Liu, J. Hierarchical management control based on equivalent fitting circle and equivalent energy consumption method for multiple fuel cells hybrid power system. *IEEE Trans. Ind. Electron.* **2020**, *67*, 2786–2797.
21. Ravey, A.; Blunier, B.; Miraoui, A. Control strategies for fuel-cell-based hybrid electric vehicles: From offline to online and experimental results. *IEEE Trans. Veh. Technol.* **2012**, *61*, 2452–2457.
22. Zhang, S.; Xiong, R. Adaptive energy management of a plug-in hybrid electric vehicle based on driving pattern recognition and dynamic programming. *Appl. Energy* **2015**, *155*, 68–78.
23. Pereira, D.F.; Lopes, F.D.; Watanabe, E.H. Non-linear model predictive control for the energy management of fuel cell hybrid electric vehicles in real-time. *IEEE Trans. Ind. Electron.* **2020**, *68*, 3213–3223.
24. Zhou, D.; Al-Durra, A.; Matraji, I.; Ravey, A.; Gao, F. Online energy management strategy of fuel cell hybrid electric vehicles: A fractional-order extremum seeking method. *IEEE Trans. Ind. Electron.* **2018**, *65*, 6787–6799.
25. Liu, C.; Murphey, Y.L. Optimal power management based on q-learning and neuro-dynamic programming for plug-in hybrid electric vehicles. *IEEE Trans. Neural Netw. Learn. Syst.* **2019**, *31*, 1942–1954.
26. Sellali, M.; Betka, A.; Djerdir, A.; Yang, Y.; Bahri, I.; Drid, S. A novel energy management strategy in electric vehicle based on H_∞ self-gain scheduled for linear parameter varying systems. *IEEE Trans. Energy Convers.* **2021**, *36*, 767–778.
27. Liu, T.; Hu, X.; Hu, W.; Zou, Y. A heuristic planning reinforcement learning-based energy management for power-split plug-in hybrid electric vehicles. *IEEE Trans. Ind. Inform.* **2019**, *15*, 6436–6445.
28. Hou, C.; Ouyang, M.; Xu, L.; Wang, H. Approximate Pontryagin's minimum principle applied to the energy management of plug-in hybrid electric vehicles. *Appl. Energy* **2014**, *115*, 174–189.
29. Ebbesen, S.; Elbert, P.; Guzzella, L. Battery state-of-health perceptive energy management for hybrid electric vehicles. *IEEE Trans. Veh. Technol.* **2012**, *61*, 2893–2900.
30. Tang, L.; Rizzoni, G.; Onori, S. Energy management strategy for HEVs including battery life optimization. *IEEE Trans. Transp. Electr.* **2015**, *1*, 211–222.
31. Zhang, S.; Hu, X.; Xie, S.; Song, Z.; Hu, L.; Hou, C. Adaptively coordinated optimization of battery aging and energy management in plug-in hybrid electric buses. *Appl. Energy* **2019**, *256*, 113891.
32. Cheng, M.; Chen, B. Nonlinear model predictive control of a power-split hybrid electric vehicle with consideration of battery aging. *ASME J. Dyn. Syst. Meas. Control* **2019**, *141*, 081008.
33. Guo, N.; Zhang, X.; Zou, Y.; Guo, L.; Du, G. Real-time predictive energy management of plug-in hybrid electric vehicles for coordination of fuel economy and battery degradation. *Energy* **2021**, *214*, 119070.
34. De Pascali, L.; Biral, F.; Onori, S. Aging-aware optimal energy management control for a parallel hybrid vehicle based on electrochemical-degradation dynamics. *IEEE Trans. Veh. Technol.* **2020**, *69*, 10868–10878.
35. Hu, X.; Zou, C.; Tang, X.; Liu, T.; Hu, L. Cost-optimal energy management of hybrid electric vehicles using fuel cell/battery health-aware predictive control. *IEEE Trans. Power Electron.* **2019**, *35*, 382–392.
36. Zhou, Y.; Li, H.; Ravey, A.; Péra, M.-C. An integrated predictive energy management for light-duty range-extended plug-in fuel cell electric vehicle. *J. Power Sources* **2020**, *451*, 227780.
37. Pasricha, S.; Shaw, S.R. A dynamic pem fuel cell model. *IEEE Trans. Energy Convers.* **2006**, *21*, 484–490.
38. Chiu, L.; Diong, B.; Gemmen, R.S. An improved small-signal model of the dynamic behavior of pem fuel cells. *IEEE Trans. Ind. Appl.* **2004**, *40*, 970–977.
39. Lukas, M.D.; Lee, K.Y.; Ghezel-Ayagh, H. Development of a stack simulation model for control study on direct reforming molten carbonate fuel cell power plant. *IEEE Trans. Energy Convers.* **1999**, *14*, 1651–1657.
40. Friede, W.; Raël, S.; Davat, B. Mathematical model and characterization of the transient behavior of a pem fuel cell. *IEEE Trans. Power Electron.* **2004**, *19*, 1234–1241.
41. Ravey, A.; Watrin, N.; Blunier, B.; Bouquain, D.; Miraoui, A. Energy-source-sizing methodology for hybrid fuel cell vehicles based on statistical description of driving cycles. *IEEE Trans. Veh. Technol.* **2011**, *60*, 4164–4174.
42. Mehdi, S.; Achour, B.; Sabrina, A.; Ouchen, S. Implementation of a real-time energy management consisting of a battery and a supercapacitor. In Proceedings of the 2017 5th International Conference on Electrical Engineering-Boumerdes (ICEE-B), Boumerdes, Algeria, 29–31 October 2017; pp. 1–6.
43. Mehdi, S.; Betka, A.; Drid, S.; Djerdir, A.; Tiar, M.; Abdedaim, S. Implementation of new adaptive power-split management strategy in a battery-super capacitor electric vehicle. In Proceedings of the 2018 International Conference on Electrical Sciences and Technologies in Maghreb (CISTEM), Algiers, Algeria, 28–31 October 2018; pp. 1–6.
44. Buller, S.; Thele, M.; de Doncker, R.W.; Karden, E. Impedance-based simulation models of supercapacitors and lithium-ion batteries for power electronic applications. *IEEE Trans. Ind. Appl.* **2005**, *41*, 742–747.

45. Wang, J.; Liu, P.; Hicks-Garner, J.; Sherman, E.; Soukiazian, S.; Verbrugge, M.; Tataria, H.; Musser, J.; Finamore, P. Cycle-life model for graphite-lifepo4 cells. *J. Power Sources* **2011**, *196*, 3942–3948.
46. Johannesson, L.; Murgovski, N.; Ebbesen, S.; Egardt, B.; Gelso, E.; Hellgren, J. Including a battery state of health model in the hev component sizing and optimal control problem. *IFAC Proc. Vol.* **2013**, *46*, 398–403.
47. He, J.; Wei, Z.; Bian, X.; Yan, F. State-of-health estimation of lithium-ion batteries using incremental capacity analysis based on volt-age-capacity model. *IEEE Trans. Transp. Electrification* **2020**, *6*, 417–426.
48. Perez, H.E.; Hu, X.; Dey, S.; Moura, S.J. Optimal charging of li-ion batteries with coupled electro-thermal-aging dynamics. *IEEE Trans. Veh. Technol.* **2017**, *66*, 7761–7770.
49. Panigrahi, D.; Chiasserini, C.; Dey, S.; Rao, R.; Raghunathan, A.; Lahiri, K. Battery life estimation of mobile embedded systems. In Proceedings of the VLSI Design 2001. Fourteenth International Conference on VLSI Design, Bangalore, India, 7 January 2001; pp. 57–63.
50. Marano, V.; Onori, S.; Guezennec, Y.; Rizzoni, G.; Madella, N. Lithium-ion batteries life estimation for plug-in hybrid electric vehicles. In Proceedings of the 2009 IEEE Vehicle Power and Propulsion Conference, Dearborn, MI, USA, 7–10 September 2009; IEEE: Manhattan, NY, USA, 2009; pp. 536–543.
51. Morales-Morales, J.; Cervantes, I.; Cano-Castillo, U. On the design of robust energy management strategies for fchev. *IEEE Trans. Veh. Technol.* **2014**, *64*, 1716–1728.